






Progress on Land Surface Phenology Estimation with Multispectral Remote Sensing

Irini Soubry¹(✉) , Ioannis Manakos² , and Chariton Kalaitzidis³ 

¹ Department of Geography and Planning, University of Saskatchewan, Saskatoon, SK S7N5C8, Canada

irini.soubry@usask.ca

² Information Technologies Institute, Centre for Research and Technology Hellas, 57001 Thessaloniki, Greece

imanakos@iti.gr

³ Department of Geoinformation in Environmental Management, Institute of Chania, Mediterranean Agronomic, 73100 Crete, Greece

chariton@maich.gr

Abstract. Phenological information can shed more light on the spatiotemporal biological processes that occur in vegetation communities. It facilitates ecosystem and resources management, conservation, restoration, policy and decision-making on local, national, and global scales. Vegetation phenology relates, among others, to the seasonal growth stages of flowering and leaf fall of specific species on the ground and is different from Land Surface Phenology (LSP), which looks at the spatiotemporal vegetation development of the land surface as measured by satellite sensors. There is a wide range of Earth Observation datasets and methods to estimate LSP. This paper reviews current progress in LSP estimation with multispectral sensing for natural and semi natural environments. It includes the satellite sensors' capacity to capture LSP, data fusion techniques, synergies, and cloud computing, machine learning, and data cube processing. One section is dedicated to the validation of LSP products and its challenges. Lastly, a short review on existing ground phenology networks, open-source software tools, and global LSP products is provided.

Keywords: Land surface phenology · Multi-source data fusion · Time series analysis · Phenology metrics · Phenology validation · Phenology networks · Global phenology products

1 Introduction

Plant and animal growth cycles are changing continuously in response to their environment. Quantitative evidence about the pulsing of the vegetation cover over terrestrial biomes provides an insight about climate change, desertification, or land use changes. Vegetation phenology refers to the changes in seasonal patterns of natural phenomena on the land, e.g. leaf out, flowering, leaf browning and fall, influenced by annual and seasonal fluctuations of biotic and abiotic (e.g. temperature, day length, precipitation)

drivers [1, 2]. Plant phenology is controlling net primary productivity, as well as seasonal fluxes of water, energy, and CO₂ between land and atmosphere [3].

On a regional level, agencies and organizations need phenology information to evaluate their conservation goals, and to conduct assessments related to the vulnerability and the potential adaptation of the region. On a national scale, phenology dates are helpful to the environmental protection agencies, as indicators of seasonal weather change impacts. Lastly, if the trend related to the impact of seasonal weather changes on specific phenology cycle metrics is significant on a global level, atmospheric scientists and the Intergovernmental Panel on Climate Change could consider season length or seasonal photosynthesis as contributing information in understanding atmospheric circulation patterns [4].

The main drivers of vegetation phenology are related to climate and vary across ecoregions [5]. In temperate regions like Central Europe, temperature is the main driver [6, 7]. In dry and semi-dry climates, water availability, soil moisture and precipitation [8] are of major importance [7, 10, 11]. This paper reviews phenology monitoring in natural and semi-natural vegetation. By semi-natural vegetation, one means vegetation that includes “extensively managed grasslands, agro-forestry areas and all vegetated features that are not used for crop production” [11]. Specifically, this paper looks at the study of Land Surface Phenology (LSP), which is the study of the spatiotemporal vegetation development of the land surface as measured by satellite sensors, and is different from species-specific phenology observed on the ground [12, 13]. LSP represents the aggregated dynamics of multiple individual organisms in every remote sensing pixel, mixed with other land covers; therefore, it is considered essentially distinct to *in situ* measurements of single organisms [14, 15].

LSP science has developed immensely in the last two decades. Past reviews tackle LSP methods and their limitations [32, 33], LSP products [34, 35], phenology networks [35, 36], and challenges that arise in LSP of optical remote sensing [35–38] separately. This review reports the recent advances and future trends for LSP retrieval of natural and semi-natural vegetation with multispectral sensors. A shorter version was published in the proceedings of the 7th International Conference on Geographical Information Systems Theory, Applications and Management [38]. This version provides more detail on the state of the art of LSP estimation, including multispectral sensors, data fusion, synergies, software tools, products, and networks. It also adds an important section related to the validation of LSP products.

2 Current Sensor Advances

Phenology cycles can be approximated from spaceborne time series of vegetation indices (VIs) [9]. Remote sensing, “the acquisition of information about the state and condition of an object through sensors that do not touch it” [16], is used for that goal. Over the years, global spaceborne phenology products based on LSP have been developed [18–21] through remote sensors that can approximate LSP. LiDAR [21], SAR [22, 23], passive microwave remote sensing [24, 25], and fluorescence remote sensing systems [26] have been used for LSP estimation. However, the use of multispectral remote sensing is more common because different phenological stages can be detected with multispectral sensors

from changes in vegetation pigments. Here, we focus on current and future multispectral remote sensing missions for LSP estimation (Table 1).

AVHRR has been used to study vegetation fluxes [10] and LSP trends [15]. Improvements to its coarse spatial resolution (1.1 to 8 km) came with MODIS, which is still being used to assess spatio-temporal LSP patterns [39, 40]. The VIIRS LSP product follows-up the MODIS product, and is being used for global LSP estimation [41, 42].

LSP can also be estimated from geostationary satellites, such as the SEVIRI sensor, which has been used to assess LSP in the studies of [54] and [55]. Recent studies used AHI on the geostationary Himawari-8 satellite to estimate LSP over the Asian-Pacific region [57, 59], and to study the sun-angle effects on LSP [58].

When looking at moderate resolution multispectral sensors, Landsat facilitates the identification of regional alterations caused by the abundance of various plant species [61] and the registration of LSP variations set by micro-climatic and topographic effects. The heterogeneity in land cover classes within each pixel is low, allowing for better field matching. Landsat's 40-year continuity currently gives room for large opportunities in LSP time series development when combined with cloud-computing and machine learning in image processing (see Sect. 5.1). The recent launch of Landsat 9 on 27 September of 2021 and initial thoughts on Landsat 10 including new imaging technologies, international collaborations, and inclusion of the commercial sector, will preserve data continuity [82].

The spatio-temporal resolution of Landsat is in many cases still too coarse for fine scale LSP estimation. Therefore, new approaches of satellite constellations are employed to increase these resolutions. The Sentinel-2 MultiSpectral Instrument (MSI) improves the temporal and spatial coverage of Landsat and is used for LSP extraction [67, 68]. Sentinel-2 and Landsat data complement each other, enabling integration [83]. They generate an average temporal overpass of 2.9 days [84], maximizing the chances of cloud-free surface data for LSP estimation.

Very high spatial (<10 m) and temporal resolution data from commercial satellite sensors can improve LSP estimation even more. PlanetScope was used for phenology estimation in semi-arid rangelands and showed promising results [71]. Most of its applications for phenology monitoring are related to agriculture [73, 74]. VEN μ S has also been used for LSP studies related to crop phenology, such as the optimization of crop emergence estimation [78], or the simulation of its bands for maize yield estimation through phenology [79]. Transformation functions between Sentinel-2 and VEN μ S surface reflectance allow for their combination into one dense time-series for vegetation monitoring [80]. Nevertheless, VEN μ S only covers selected sites on the globe [85].

New satellite sensors scheduled to launch will support LSP monitoring. The JPSS mission, that carries the VIIRS instrument, will launch three spacecrafts between 2021 and 2031 [86]. Meanwhile, the Planetscope nanosatellite constellation is launching continuously every three to six months. In the end, this will result in daily images of the entire globe at very high spatial resolution (3m approximately) [87].

Table 1. Satellite sensor characteristics for LSP (Land Surface Phenology) studies and example applications. Source: [38].

Satellite sensor	Orbit-type	Operation timespan	Spatial resolution	Temporal resolution	Example LSP applications	Relevant studies	Data Source
AVHRR	Sun-synchronous	1978-Present	1.1 km at nadir	Daily	global LSP trends;	[11, 16, 44]	[44]
MODIS	Sun-synchronous	1999-Present	250 m, 500 m, 1 km	Daily	global LSP trends;	[3, 15, 35, 40, 41, 46–50]	[50]
VIIRS	Sun-synchronous	2011-Present	375 m, 250m, 750 m	Daily	global LSP trends, comparison of global products, comparison with ground phenology;	[42, 43, 52, 53]	[53]
SEVIRI	Geostationary	2002-Present	1 km, 3 km	15 min	regional LSP trends;	[54, 55]	[56]
AHI	Geostationary	2014-Present	500 m, 1 km, 2 km	10 min	regional LSP trends;	[58–60]	[60]
Landsat	Sun-synchronous	1972-Present	30 m, 80 m	16-days, 18-days	LSP trends, comparison with ground phenology, land cover characterization;	[62–65]	[65]
Sentinel-2	Sun-synchronous	2015-Present	10 m, 20 m, 60 m	5-days, 10-days	LSP trends, comparison with ground phenology;	[67–70]	[70]
PlanetScope	Sun-synchronous	2009-Present	3.7 m at nadir	Daily	LSP trends in agriculture;	[72–75]	[76–78]
VENμS	Sun-synchronous	2017-Present	3 m, 5.3 m	2-days	LSP trends in agriculture;	[79–81]	[81]

3 LSP Estimation Using Multi-Source Earth Observation

A composite cloud-free image utilizes cloud-free parts of images of close dates [89]. These type of images are produced from AVHRR, MODIS, and SPOT data to account for cloud cover. One drawback of this method is that the temporal frequency of the data, required for LSP, is lower. On the other hand, data fusion or blending of satellite data from different sensors can generate synthetic information of high spatiotemporal resolution [90]. Also, synergies between satellite products, such as Sentinel-2 and Landsat-8 can be used to densify time series. In this case, each product of the synergy remains unchanged. Data fusion and synergies facilitate LSP estimations with their high temporal and spatial resolution, allowing for detailed phenology cycles. Examples of recent data integration methods are included in Table 2.

Efforts have been made to extract medium resolution (MR) (10–100 m) LSP metrics through various data fusion methods. FORCE ImproPhe allows for the prediction of MR LSP based on corresponding coarse resolution (0.1–2 km) LSP [91]. Information from the local pixel neighborhood from both sources is obtained, and spectral distance and multiscale heterogeneity metrics are used as predictor variables. Another approach

Table 2. Examples of satellite data integration methods (i.e. data fusion and synergies). Adapted from [38].

Data integration method	Satellite sensor combinations	Details	Source
FORCE ImproPhe	MODIS, Landsat, Sentinel	Uses local pixel neighborhood, denoises LSP, preserves sharp edges	[92–94]
Multi-year high resolution data composition	Landsat	Accounts for higher spatial heterogeneity	[94]
Automatic co-registration	Landsat, Sentinel	Co-registration of Landsat-8 to Sentinel-2A & Sentinel-2A to Sentinel-2B	[95]
Assisted downscaling	Landsat, Sentinel	Downscales Landsat-8 to Sentinel-2 resolution	[84]
Super-resolution enhancement	Landsat, Sentinel	Uses convolution neural networks trained with Sentinel-2 data	[29]
HLS	Landsat, Sentinel	A combined Landsat/Sentinel product	[96, 97]

synthesizes multiple years of medium resolution data into a single LSP curve. This method was used with a 32-year Landsat time series to define the growing season in the forests of the Northern Hemisphere [94]. Nijland et al. [98] used the same approach to extract average yearly LSP curves in mixed stands and conifer forests of Rocky Mountains (CA) from 1984 to 2014.

Other studies that address vegetation seasonality evaluate the juxtaposition of Sentinel-2 and Landsat-8 products [99, 100]. Due to differences between the two sensors, cross-calibration is needed for their integration, such as automatic co-registration [95], assisted downscaling [28], and super-resolution enhancement [29]. In these studies, the replacement of the NIR band with the first red-edge Sentinel-2 band has shown to provide better comparisons with Landsat data, since its range is more similar to the Landsat NIR band [101, 102].

Lastly, a synergy between Landsat 8 and Sentinel-2 was developed through the Multi-source Land Imaging (MuSLI) program of NASA [101]. This product is the Harmonized Landsat Sentinel-2 (HLS) dataset. It is a global product that provides land surface observations every 2 to 3 days at 30 m spatial resolution [103], and has been used for the development of an operational LSP product [104]. The combination of these satellite sensors generates time series with unprecedented frequency. However, one should be aware of the various theoretical and technical hurdles when using different sensor constellations.

4 Validation of LSP Products

Multiple satellite missions and new image processing technologies arose in recent years, allowing for higher spatial and temporal resolution of data individually, or through fusions and synergies [28–30]. Moving to a finer scale helps unfold local structures associated with microclimate, species distribution and composition, disturbance factors, and land utilization. Nevertheless, phenological ground observations are required to validate the results obtained from spaceborne products' estimations [30]. Validation of LSP results encompasses many challenges and still remains an active research topic [31, 32].

Plot scale phenology usually measures individual species. LSP observations are maximum value composites with a regular observation interval derived from a specific observation period, generated from irregular observation intervals collected from satellite remote sensing. In several studies the LSP changes that were observed through remote sensing were greater than the ones in ground phenology data [3, 32, 41, 47]. The seasonal patterns detected from Earth observation data cannot be linked 1:1 to actual differences in vegetation phenology [32], and their accuracy could vary between ecosystems [105]. To link LSP estimations with ground phenology observations one should understand the species composition in the study area [48]. Simultaneous field-based and RS data are needed along different stages of multiple growing seasons [14]. After this, up-scaling can be done by combining field observations with a high-resolution satellite image, to produce a higher resolution map of the field parameter that was observed. This map can then be compared to the medium resolution satellite data [106]. Overall, it is important for users to be aware of the data product limitations, so as not to be led to inaccurate and misleading phenology monitoring.

4.1 Ground Phenology Monitoring

Detailed ground phenology information is most commonly acquired as point measurements in random spatial patterns, and phenological stages are registered in standardized numeric codes [107]. The main downside of plot scale phenological data is that it is time- and resource-consuming, localized, and observes a small sample of species [48]. Therefore, several countries use crowd-sourcing to obtain such information. Current methods used for the retrieval of ground phenology data include:

- phenology diary reports of ground observation sites; for example, the USA National Phenology Network (USA-NPN) created the National Phenology Database (NPDb) that contains data collected from scientists and trained volunteers; it is comprised of field-based observations of plants and animals [4]); also the BBCH (Biologische Bundesanstalt, Bundessortenamt und CHemische Industrie) scale is a uniform coding system (from 0 to 10) of phenologically similar growth stages among plants that is being used for ground phenology monitoring [108, 109];
- optical phenology towers to generate vegetation greenness indices close to the surface with high temporal resolution [31, 105]; these towers have in most cases ground-based visible spectrum digital cameras to monitor vegetation development with repeating photography during the growing season [64, 98];

- ground radiometric measurements with a handheld radiometer of crop canopies during the growing season to define a semi-empirical model for the time profile of the vegetation index for each crop at the regional scale [47, 110];
- gross primary production (GPP) retrieved from a flux tower observation network [3, 110];
- air temperature records [105].

Recently, improved alternative ground-based LSP validation methods are being used at ground networks around the globe. Examples include ground-based phenological cameras, *in situ* forest canopy greenness indices from phenology towers, and flux-measured GPP. The Society of Biometeorology Phenology Commission (ISB-PC) and the World Meteorological Organization Commission for Agricultural Meteorology (WMO-CAGM) built a Global Alliance of Phenological Observation Networks (GAPON) [2]. The phenology networks in this community are up to date 53 in number, and include –among others- nationwide approaches. Examples of large phenological networks are provided in Table 3.

4.2 Ground Reference vs. Ground Truth Data

Ground phenological observations differ from estimations of biophysical parameters, such as ground spectral measurements or LSP, and are mostly related to the subjective decision of the data collector. Different individuals can give different phenology dates for the same sampling site and, as a result, ground data collection relies heavily on the collector’s experience and knowledge. However, precise instructions, such as the use of the BBCH scales [108] with photo examples could help the observer. Nevertheless, it is not so straightforward to select a derived LSP method, which will match precisely with ground phenology (GP) data. In reality, collecting extensive *in situ* measurements at the same frequency of LSP data is problematic for common small research teams consisting of a few scientists and students [14].

Moreover, according to Rankine et al. [31], simultaneous multi-annual observations of vegetation greenness from satellite and near-surface observations are not so common due to the challenges that exist in relation to implementing and maintaining sensitive radiometric instrumentation. They believe that another factor that limits direct comparisons between GP and LSP is the spectral bands adopted to construct the VI. Narrowband and broadband vegetation indices have different sensitivity to alterations in leaf area and chlorophyll content.

Another issue is the way in which the Start of Season (SOS) is defined. This can be different, depending on the method used for LSP extraction [34]. The results of Wu et al. [46] showed that the modelled SOS outputs tend to appear on earlier dates than the ground observations, irrespective of the method used to model the metric. This is also consistent with the scaling study of Zhang et al. [115], where the earlier SOS pixels define the SOS detection at coarse resolution more than the later SOS pixels of an area. Interestingly, it has been found that SOS at coarser resolution (i.e. 500 m), corresponds to vegetation green up of 30% of the total pixel area, despite the variation in SOS dates within [115]. One reason could be that different LSP-SOS metrics represent different ground phenology-SOS observations [48]. Similar difficulties arise when trying

Table 3. Major existing phenology networks. Information retrieved from GLOBE [20], Nasa-hara & Nagai [111], NEON [18], PEN [112], PEP725 [19], Templ et al. [113], USA-NPN [17], PHENOCAM [114]. Source [38].

Phenology Networks	Purpose	Users	Collaborations	Extra information
USA-NPN	Collect, store, distribute phenology data	Researchers, natural resource managers, policy-makers, educators, citizen scientists, NGO's	-NEON; -Nature's Notebook	Standardized plant & animal observation protocols
NEON	Collect ecological data: <i>in situ</i> measurements/ observations & airborne remote sensing surveys	Researchers	-81 field sites in US	175 open access products
PEP725	Open access database to facilitate phenological research, education, environmental monitoring	Researchers, educators	-7 phenology network partners; -32 European meteorological services	-Volunteer data collected from 1868 to present; -12 million records
GLOBE	International science and education program to promote teaching and learning of science	Students, educators	-NASA, NSF, NOAA; -121 countries	Over 150 million ground biophysical measurements
PEN	Validate terrestrial RS products of ecology, phenology changes	Ecologists, remote sensing specialists, scientists, citizens	-FluxNet, ILTER, AsiaFlux -38 sites worldwide, most in Japan	Some sites measure environmental ecophysiological properties
PhenoCam	For phenological model validation, evaluation of satellite RS products, studies of climate change impacts on terrestrial ecosystems	Researchers, remote sensing specialists	-750 sites across North America	Data derived from visible-wavelength digital camera imagery

to define the End of Season (EOS). This is because plant canopy greenness changes gradually in autumn. EOS estimation becomes even harder for evergreen species, for which the greenness changes only slightly [131]. Therefore, small differences of EOS between years are even more difficult to detect accurately using remote sensing data [46]. Therefore, it is important to implement standardized protocols for ground phenology monitoring [116], as well as for LSP metrics extraction. An effort towards that direction, as far as ground phenology monitoring is concerned, has resulted in the plant phenology monitoring design of NEON [117]. Unfortunately this has not yet been implemented with consistency around the globe [117], which is why studies that integrate field-based validation vary [31, 98].

4.3 Spatial Cross-Scale Issues

While being very valuable, field measurements often represent a small area and are in most cases subjective, because of the approach being used [98]. Up until now it has not been an easy task to match field and satellite-based observations because of the difficulty to transpose these measurements to the same scale and because of the use of phenological metrics that are approximations of the phenophases [106]. The spatial mismatch between the field-based point measurements of plots and the resolution of satellite pixels at local scales, particularly medium resolution data, further complicates the process [61]. This happens because most field data are usually species-specific and observed at scales that are incompatible with medium resolution remote sensing observations.

More specifically, this relates to the issue of scale mismatch due to vegetation heterogeneity [118]. It is rare for vegetation to be uniform in the Landsat or Sentinel-2 resolution, whereas in field observations, budburst or flowering stages are identified for a small amount of plants in each sampling plot. Thus, relating *in situ* phenological events with the mean LSP of a Landsat or Sentinel-2 pixel is difficult, as these pixels are spectrally mixed [31]. Furthermore, in cases of mixed pixels containing vegetated and non-vegetated areas, the interpretation of the LSP metrics' biophysical meaning could be misleading. In these cases, the LSP metrics could indicate phenology change in the LSP curve, even if in reality it is indicating a change in the ratio of vegetation/ non-vegetation in the monitored area [119]. Wrong assumptions about the homogeneity of a region can also be made. For example, a forest can still have heterogeneous LSP due to species distribution and microclimatic conditions [115]. As a result, even homogeneous plots of the same species can reveal phenology variability caused by differences in site conditions or ecotope.

Moreover, the timing of green-up that is extracted from satellite time-series is often more related to understory canopy than to overstory [120]. For instance, during early and in-between growing stages in a tropical dry forest the understory vegetation develops its leaves as a response to the first rains in the beginning of the growing season [31]. These misinterpretations can be circumvented by visually inspecting vegetation structures and categories in the study area with the use of very high resolution images (e.g. Google Earth images) or *in situ* data [106]. Nevertheless, alternative approaches have proposed to scale-up species-specific field-based measurements to the landscape scale with the introduction of the Landscape Phenology Index, allowing for comparability with 250 m to 1 km LSP products [121]. This index utilizes the phenocluster concept,

by aggregating community phenologies (individual phenologies of the same species that cover a representative population phenology area), and is an area-weighted average of all community phenologies over the area of study [121].

4.4 Temporal Scale Issues

Most of the disagreement between ground phenology and LSP is connected to the lower temporal resolution of the remote sensing product. Large data gaps in a time series could result in lower accuracy during interpolation. Particularly, when canopy growth or senescence is rapid, low temporal resolution products cannot accurately detect the transition dates [31]. Additionally, when field-observed phenological stages correspond to very subtle differences, these might not be detectable in satellite-measured LSP due to spectral and temporal deficiencies of satellite data. For instance, as pointed out in the study of Misra et al. [48], bud break is measured in ground phenology, but is reported as undetectable in LSP because this phenomenon is spatially too small to sufficiently influence the signal in the NIR band of a satellite sensor. In addition, bud burst signals intermixed with pre-existing understory could also contribute to the poor detection of early phenophases [48]. This is why LSP mainly focuses on phenophases that can be detected and allow for scaling up. Since ground phenology and land surface phenology have different definitions, it is almost impossible to get perfect temporal alignment in terms of specific day of the year. However, the general patterns at the start of the season as observed by field and satellite measurements are assumed to have a moderate relation, because they both look at the starting points in the cycle of vegetation development [48]. Nevertheless, one must acknowledge that in these type of comparisons, one is trying to compare a spatial integral with observations of individual plants of single species or even only traits thereof.

5 Recent LSP Advances, Tools and Products

5.1 New Trends and Advances

Cloud computing (CC) and machine learning allow for faster processing in LSP retrieval. This is especially advantageous when dealing with big data of satellite imagery, which demand for high-performance processes that are not available from a single computer. CC transfers the image processing from a scientist's personal computer to an online server. Time series from all available satellite image scenes can be easily generated through CC. For instance, the Google Earth Engine (GEE) server has been used to retrieve LSP over the North Hemisphere from VEGETATION and PROBA-V time series [122]. Other studies that estimated LSP through GEE include those of Li et al. [123], Venkatappa et al. [124], and Workie and Debella [125]. Freely accessible cloud computing platforms apart from GEE include Amazon Web Services (AWS) Open Data, TerraScope Virtual Machine, and the 'PhenologyMetrics' algorithm (see Sect. 5.2).

In addition, data cube technologies have become popular for processing remote sensing data. Image data cubes are "large collections of temporal, multivariate datasets typically consisting of analysis ready multispectral Earth observation data" [126]. The

Committee of Earth Observation Satellites (CEOS) created Open Data Cube to accommodate this concept. Data cubes can be used for LSP estimation. Li et al. [127] used this technology to study changes in vegetation green-up dates. Data cubes allow for the inclusion of all available imagery over very large extents. This can generate temporally detailed and geographically expansive LSP estimations.

Similarly, machine-learning techniques allow for the incorporation of very large data inputs. There is potential for machine learning to be used with data cubes and multi-source earth observation data. Until now, machine learning has been applied to predict ground-based phenophases or LSP from daily pheno-tower data. In detail, it has been used to learn and detect phenological patterns in numerous ground digital images [128, 129], and to fill spatiotemporal ground-based phenology to help forecast LSP with remote sensing and meteorological data [130]. The last study showed moderate-to-high potential for LSP estimation with RS through machine learning. The advantages of machine learning for LSP estimation were included in the DATimeS software (developed in 2019), with twelve machine learning fitting algorithms for time series analysis of phenology data (see Sect. 5.2). Machine learning techniques that enhance LSP are just starting to gain more ground.

Lastly, as seen previously, one of the long-standing difficulties in LSP estimation was, until recently, the accurate determination of EOS phenology metrics. One solution is to take an ensemble approach, such as taking the average of two methods. Yuan et al. [132] applied this technique by averaging the result of the midpoint and double logistical fitting to determine EOS. Moreover, it was recently discovered that for an accurate estimation of autumn phenology one needs to combine sensors and satellite data. Lu et al. [133] found that autumn phenology derived from fluorescence satellite data had higher correspondence with gross primary production (GPP) autumn phenology than autumn phenology derived from vegetation indices. Wang et al. [134] found similar results, where the EOS was estimated earlier with fluorescence satellite data data, followed by NDVI and vegetation optical depth estimations. This means that photosynthetic activity decreases before any changes in leaf color can be detected, and that the decrease in vegetation water content is the last stage of senescence. These results were consistent globally and shed light on the underlying structural and functional processes of autumn senescence.

5.2 Open-Source LSP Software

There are a number of open-source LSP estimation software. TIMESAT is a software package that enables the extraction of seasonality parameters. Its most recent version includes “Seasonal and Trend decomposition using Loess” (Version 3.3, 2017) [135], and plans the incorporation of Landsat and Sentinel-2 data [9]. PhenoSat produces LSP information from vegetation index time series. It has seven different smoothing algorithms, it recognizes more than one growth season in each year, and can focus on periods within a season [136, 137]. Verbesselt et al. [138] developed the “Breaks For Additive Seasonal Trend” method to extract seasonal and trend elements from time series to detect vegetation greenness. Examples include its use to determine grassland trends and phenology of the Flint Hills ecoregion [139], or to examine seasonal trends of vegetation on military training grounds [140]. Further, Frantz et al. [91] created the “Spline analysis

of Time Series” algorithm to derive LSP by fitting spline models to remotely sensed time series. Twenty metrics per pixel are generated and relate to specific dates, and the length and amplitude of seasons. The Joint Research Centre provides “Software for the Processing and Interpretation of Remotely Sensed Image Time Series”, through which LSP SOS and EOS are calculated from 10-day composite images for both single and double growing seasons with the threshold technique [142–146]. Forkel et al. [146, 147] created functions to analyse seasonal trends and trend changes in Earth Observation time series with the ‘greenbrown’ package in R [148]. Also, the ‘phenex’ package in R has functions for analysis of LSP data [149]. Lastly, the Ecopotential Virtual Library packaged the ‘phenex’ algorithm in an online workflow (“Estimation of phenology metrics – PhenologyMetrics”) created by the Centre for Research and Technology Hellas [150]. It can derive three LSP metrics from NDVI time series during vegetation growth. The advantages include the estimation of multiple vegetation cycles in a growing period [151] and online processing without the need for high processing capabilities.

5.3 Global LSP Products

Some of the global LSP products are the MODIS Land Cover Dynamics product (MCD12Q2), the VIIRS Global Land Surface Phenology (GLSP) product, and the Vegetation Index and Phenology (VIP) Phenology (VIPPHEN) global product, which produce yearly LSP metrics (see Table 4).

Table 4. Global LSP products: MODIS Land Cover Dynamics product (MCD12Q2), VIIRS Global Land Surface Phenology product (GLSP), Making Earth System Data Records for Use in Research Environments (MEaSUREs) Vegetation Index and Phenology (VIP) global dataset. Information retrieved from Gray et al. [152], USGS [153], and X. Zhang, Liu, et al. [42]. Source [38].

Global LSP products	Timespan	Source	Spatial Resolution
MCD12Q2	2001 to end 2017	EVI2 from MODIS BRDF Adjusted Reflectance (NBAR)	500 m
VIIRS GLSP	2012 to Present	EVI2 from daily VIIRS BRDF NBAR	500 m
MEaSUREs VIP	1981 to end 2014	NDVI and EVI2 from AVHRR N07, N09, N11, N14 datasets from 1981–1999; MODIS Terra MOD09 Surface Reflectance from 2000–2014	5600 m
HLS	2013 to Present	Surface Reflectance and Top of Atmosphere brightness data from Landsat 8 and Sentinel-2A and Sentinel-2B	30 m

The MCD12Q2 product is an LSP product that provides global LSP metrics derived from satellite image time series. If values are missing in an area due to cloud cover

or other causes, the gaps are filled with good quality values from the year before or the following [152]. This product can be used in areas with two growing seasons [34]. The VIIRS LSP product can also estimate phenology for various vegetation types and climate systems [42]. The MEaSUREs VIP product is defined with a moving average window of three years in order to eliminate noise, and is accompanied with a reliability value to help determine data quality [153]. Lastly, the HLS surface reflectance dataset [154] currently has global coverage and can be used to derive LSP time series with observations available every 2 to 3 days [103].

6 Conclusions

This review pointed out that the use of multi-source Earth observation data, such as the HLS product, can reduce limitations that are connected to the spatial and temporal resolution of LSP. Medium spatial resolution LSP products will be more accurate at a temporal resolution of less than 16 days. Moreover, the EOS is harder to estimate from remote sensing data because canopy greenness diminishes gradually during autumn, making the transitions not very apparent. However, combined use of optical, microwave, and fluorescence RS could provide better insight to this phenomenon.

This review also showed that validation efforts should ideally include sites at least equal to the pixel size of the sensor in order to reduce the observers' subjectivity and the uncertainties of the measurements. However, the sensor's pixel size can cover a large area on the ground, making frequent site visits particularly unfeasible. Drone-mounted cameras could potentially provide a solution to this issue. Generally, studies should use phenology towers or mounted digital cameras to reduce the validation workload; mainly, because traditional field work for the collection of phenology data is often very hard to conduct for small science teams. In addition, researchers should be aware of the plant species composition in a mixed pixel, to better understand the VI response.

Lastly, Earth observation time series of higher spatial and temporal resolution bring a multitude of opportunities. Monitoring vegetation at individual stands could become possible. Large amounts of Earth observation data ask for high-performance processing methods; however cloud solutions for data storage and processing as well as machine learning workflows are freely accessible, facilitating big data processing. Moreover, data cubes allow for a new viewpoint on data analysis. This makes the previous technologies suitable for LSP estimation. Overall, the recent progress and future prospects of LSP estimation with multispectral remote sensing reviewed in this article will be able to support several of the United Nations Sustainable Development Goals and the Aichi Biodiversity Targets through developing Essential Biodiversity Variables that correspond to the Group on Earth Observation initiatives.

Acknowledgements. The authors acknowledge valuable suggestions and support from Giorgos Kordelas and George Kazakis. This review study has been partially funded and supported by the European Union's Horizon 2020 Coordination and Support Action under Grant Agreement No. 952111, EOTiST (<https://cordis.europa.eu/project/id/952111>).

References

1. Lieth, H.: Purposes of a phenology book. In: Lieth, H. (ed.) *Phenology and Seasonality Modeling*. Ecological Studies, vol. 8, pp. 3–19. Springer, Heidelberg (1974). https://doi.org/10.1007/978-3-642-51863-8_1
2. USA-NPN: Phenology Networks around the World. <https://www.usanpn.org/partner/gapon> (2020). Accessed 14 Jan 2020
3. Karkauskaite, P., Tagesson, T., Fensholt, R.: Evaluation of the plant phenology index (PPI), NDVI and EVI for start-of-season trend analysis of the Northern Hemisphere boreal zone. *Remote Sens.* **9**, 1–21 (2017). <https://doi.org/10.3390/rs9050485>
4. Rosemartin, A.H., Crimmins, T.M., Enquist, C.A.F., et al.: Organizing phenological data resources to inform natural resource conservation. *Biol. Conserv.* **173**, 90–97 (2014). <https://doi.org/10.1016/j.biocon.2013.07.003>
5. Munson, S.M., Long, A.L.: Climate drives shifts in grass reproductive phenology across the western USA. *New Phytol.* **213**, 1945–1955 (2017). <https://doi.org/10.1111/nph.14327>
6. Arfin Khan, M.A.S., Beierkuhnlein, C., Kreyling, J., et al.: Phenological sensitivity of early and late flowering species under seasonal warming and altered precipitation in a semiarid temperate Grassland ecosystem. *Ecosystems* **21**, 1306–1320 (2018). <https://doi.org/10.1007/s10021-017-0220-2>
7. Zhao, J., Wang, Y., Zhang, Z., et al.: The variations of land surface phenology in Northeast China and its responses to climate change from 1982 to 2013. *Remote Sens.* **8**, 1–23 (2016). <https://doi.org/10.3390/rs8050400>
8. Sousa, D., Small, C., Spalton, A., Kwarteng, A.: Coupled spatiotemporal characterization of monsoon cloud cover and vegetation phenology. *Remote Sens.* **11**, 1–22 (2019). <https://doi.org/10.3390/rs11101203>
9. Kuenzer, C., Dech, S., Wagner, W.: Remote Sensing Time Series. *Remote Sensing and Digital Image Processing*, pp 225–245 (2015). <https://doi.org/10.1007/978-3-319-15967-6>
10. Bradley, B.A., Jacob, R.W., Hermance, J.F., Mustard, J.F.: A curve fitting procedure to derive inter-annual phenologies from time series of noisy satellite NDVI data. *Remote Sens. Environ.* **106**, 137–145 (2007). <https://doi.org/10.1016/j.rse.2006.08.002>
11. García-Feced, C., Weissteiner, C.J., Baraldi, A., et al.: Semi-natural vegetation in agricultural land: European map and links to ecosystem service supply. *Agron. Sustain. Dev.* **35**, 273–283 (2014). <https://doi.org/10.1007/s13593-014-0238-1>
12. de Beurs, K.M., Henebry, G.M.: Land surface phenology, climatic variation, and institutional change: analyzing agricultural land cover change in Kazakhstan. *Remote Sens. Environ.* **89**, 497–509 (2004). <https://doi.org/10.1016/j.rse.2003.11.006>
13. de Beurs, K.M., Henebry, G.M.: Land surface phenology and temperature variation in the International Geosphere-Biosphere Program high-latitude transects. *Glob. Change Biol.* **11**, 779–790 (2005). <https://doi.org/10.1111/j.1365-2486.2005.00949.x>
14. Elmore, A.J., Stylinski, C.D., Pradhan, K.: Synergistic use of citizen science and remote sensing for continental-scale measurements of forest tree phenology. *Remote Sens.* **8**, 1–16 (2016). <https://doi.org/10.3390/rs8060502>
15. Wang, Y., Zhao, J., Zhou, Y., Zhang, H.: Variation and trends of landscape dynamics, land surface phenology and net primary production of the Appalachian Mountains. *J. Appl. Remote Sens.* **6**, 061708 (2012). <https://doi.org/10.1117/1.jrs.6.061708>
16. Chuvieco, E.: *Fundamentals of Satellite Remote Sensing: An Environmental Approach*, 2nd edn. Taylor & Francis (2016)
17. USA-NPN: USA National Phenology Network (2019). <http://dx.doi.org/10.5066/F7XDOZRK>. Accessed 17 Sept 2019

18. NEON: NEON Science-About (2019). <https://www.neonscience.org/about>. Accessed 6 Nov 2019
19. PEP725: About the Pan European Phenology Project PEP725 (2019). <http://www.pep725.eu/index.php>. Accessed 26 Sept 2019
20. GLOBE: Overview - GLOBE (2019). <https://www.globe.gov/about/overview>. Accessed 26 Sept 2019
21. Salas, E.A.L.: Waveform LiDAR concepts and applications for potential vegetation phenology monitoring and modeling: a comprehensive review. *Geo-Spatial Inf. Sci.* **00**, 1–22 (2020). <https://doi.org/10.1080/10095020.2020.1761763>
22. Mascolo, L., Lopez-Sanchez, J.M., Vicente-Guijalba, F., et al.: A complete procedure for crop phenology estimation with PolSAR data based on the complex Wishart Classifier. *IEEE Trans. Geosci. Remote Sens.* **54**, 6505–6515 (2016). <https://doi.org/10.1109/TGRS.2016.2585744>
23. Cota, N., Kasetkasem, T., Rakwatin, P., et al.: Rice phenology estimation using SAR time-series data. In: 2015 6th International Conference of Information and Communication Technology for Embedded Systems (IC-ICTES), pp. 1–5 (2015)
24. Alemu, W.G., Henebry, G.M., Melesse, A.M.: Land surface phenologies and seasonalities in the US prairie pothole region coupling AMSR passive microwave data with the USDA cropland data layer. *Remote Sens.* **11** (2019). <https://doi.org/10.3390/rs11212550>
25. Dannenberg, M., Wang, X., Yan, D., Smith, W.: Phenological characteristics of global ecosystems based on optical, fluorescence, and microwave remote sensing. *Remote Sens.* **12** (2020). <https://doi.org/10.3390/rs12040671>
26. Joiner, J., Yoshida, Y., Vasilkov, A.P., et al.: The seasonal cycle of satellite chlorophyll fluorescence observations and its relationship to vegetation phenology and ecosystem atmosphere carbon exchange. *Remote Sens. Environ.* **152**, 375–391 (2014). <https://doi.org/10.1016/j.rse.2014.06.022>
27. Skakun, P.S., Ju, J., Claverie, M., et al.: Harmonized Landsat Sentinel-2 (HLS) Product User's Guide (2018)
28. Li, Z., Zhang, H.K., Roy, D.P., et al.: Landsat 15-m Panchromatic-Assisted Downscaling (LPAD) of the 30-m reflective wavelength bands to Sentinel-2 20-m resolution. *Remote Sens.* **9**, 1–18 (2017). <https://doi.org/10.3390/rs9070755>
29. Pouliot, D., Latifovic, R., Pasher, J., Duffe, J.: Landsat super-resolution enhancement using convolution neural networks and Sentinel-2 for training. *Remote Sens.* **10**, 1–18 (2018). <https://doi.org/10.3390/rs10030394>
30. Beck, P.S.A., Jönsson, P., Høgda, K.A., et al.: A ground-validated NDVI dataset for monitoring vegetation dynamics and mapping phenology in Fennoscandia and the Kola peninsula. *Int. J. Remote Sens.* **28**, 4311–4330 (2007). <https://doi.org/10.1080/01431160701241936>
31. Rankine, C., Sánchez-Azofeifa, G.A., Guzmán, J.A., et al.: Comparing MODIS and near-surface vegetation indexes for monitoring tropical dry forest phenology along a successional gradient using optical phenology towers. *Environ. Res. Lett.* **12**, 105007 (2017). <https://doi.org/10.1088/1748-9326/aa838c>
32. de Beurs, K.M., Henebry, G.M.: Chapter 9, Spatio-Temporal Statistical Methods for Modelling Land Surface Phenology. In: *Phenological Research: Methods for Environmental and Climate Change Analysis*. pp. 177–208 (2010)
33. Zeng, L., Wardlow, B.D., Xiang, D., et al.: A review of vegetation phenological metrics extraction using time-series, multispectral satellite data. *Remote Sens. Environ.* **237**, 111511 (2020). <https://doi.org/10.1016/j.rse.2019.111511>
34. Henebry, G.M., de Beurs, K.M.: Chapter 21-Remote sensing of land surface phenology: a prospectus. In: *Phenology: An Integrative Environmental Science*, pp 483–502 (2013)

35. Reed, B.C., Schwartz, M.D., Xiao, X.: Remote sensing phenology. In: Noormets, A. (ed.) *Phenology of Ecosystem Processes*, pp 231–246. Springer, New York (2009). https://doi.org/10.1007/978-1-4419-0026-5_10
36. Morisette, J.T., Richardson, A.D., Knapp, A.K., et al.: Tracking the rhythm of the seasons in the face of global change: phenological research in the 21st century. *Front Ecol. Environ.* **7**, 253–260 (2009). <https://doi.org/10.1890/070217>
37. Helman, D.: Land surface phenology: what do we really ‘see’ from space? *Sci. Total Environ.* **618**, 665–673 (2018). <https://doi.org/10.1016/j.scitotenv.2017.07.237>
38. Soubry, I., Manakos, I., Kalaitzidis, C.: Recent advances in land surface phenology estimation with multispectral sensing. In: *Proceeding of the 7th International Conference on Geographical Information Systems, Theory, Applications and Management (GISTAM 2021)*. SCITEPRESS -Science and Technology Publications, Lda, pp. 134–145 (2021)
39. Khare, S., Drolet, G., Sylvain, J.D., et al.: Assessment of spatio-temporal patterns of black spruce bud phenology across Quebec based on MODIS-NDVI time series and field observations. *Remote Sens.* **11**, 1–16 (2019). <https://doi.org/10.3390/rs11232745>
40. Cui, T., Martz, L., Lamb, E.G., et al.: Comparison of grassland phenology derived from MODIS satellite and PhenoCam near-surface remote sensing in north America. *Can. J. Remote Sens.* **45**, 1–16 (2019). <https://doi.org/10.1080/07038992.2019.1674643>
41. Moon, M., Zhang, X., Henebry, G.M., et al.: Long-term continuity in land surface phenology measurements: a comparative assessment of the MODIS land cover dynamics and VIIRS land surface phenology products. *Remote Sens. Environ.* **226**, 74–92 (2019). <https://doi.org/10.1016/j.rse.2019.03.034>
42. Zhang, X., Liu, L., Liu, Y., et al.: Generation and evaluation of the VIIRS land surface phenology product. *Remote Sens. Environ.* **216**, 212–229 (2018). <https://doi.org/10.1016/j.rse.2018.06.047>
43. Fischer, A.: A model for the seasonal variations of vegetation indices in coarse resolution data and its inversion to extract crop parameters. *Remote Sens. Environ.* **48**, 220–230 (1994). [https://doi.org/10.1016/0034-4257\(94\)90143-0](https://doi.org/10.1016/0034-4257(94)90143-0)
44. Wunderle, S., Neuhaus, C.: *AVHRR Master Data Set Handbook - Deliverable 16 (WP 7)*. Bern (2020)
45. Zhang, X., Friedl, M.A., Schaaf, C.B., et al.: Monitoring vegetation phenology using MODIS. *Remote Sens. Environ.* **84**, 471–475 (2003). [https://doi.org/10.1016/S0034-4257\(02\)00135-9](https://doi.org/10.1016/S0034-4257(02)00135-9)
46. Wu, C., Peng, D., Soudani, K., et al.: Land surface phenology derived from normalized difference vegetation index (NDVI) at global FLUXNET sites. *Agric. Meteorol.* **233**, 171–182 (2017). <https://doi.org/10.1016/j.agrformet.2016.11.193>
47. Cai, Z., Jönsson, P., Jin, H., Eklundh, L.: Performance of smoothing methods for reconstructing NDVI time-series and estimating vegetation phenology from MODIS data. *Remote Sens.* **9**, 20–22 (2017). <https://doi.org/10.3390/rs9121271>
48. Misra, G., Buras, A., Menzel, A.: Effects of different methods on the comparison between land surface and ground phenology - A methodological case study from South-Western Germany. *Remote Sens.* **8**, 1–18 (2016). <https://doi.org/10.3390/rs8090753>
49. Cui, T., Martz, L., Zhao, L., Guo, X.: Investigating the impact of the temporal resolution of MODIS data on measured phenology in the prairie grasslands. *GIScience Remote Sens.* **57**, 395–410 (2020). <https://doi.org/10.1080/15481603.2020.1723279>
50. ESA: Terra/Aqua MODIS. Earth Online (2020). <https://earth.esa.int/web/guest/missions/3rd-party-missions/current-missions/terraaqua-modis>. Accessed 8 Nov 2020
51. Zhang, X., Jayavelu, S., Liu, L., et al.: Evaluation of land surface phenology from VIIRS data using time series of PhenoCam imagery. *Agric. Meteorol.* **137–149**, (2018). <https://doi.org/10.1016/j.agrformet.2018.03.003>

52. Zhang, X., Liu, L., Yan, D.: Comparisons of global land surface seasonality and phenology derived from AVHRR, MODIS, and VIIRS data. *J. Geophys. Res. Biogeosciences* **122**, 1506–1525 (2017). <https://doi.org/10.1002/2017JG003811>
53. NASA EARTHDATA (2020) Visible Infrared Imaging Radiometer Suite (VIIRS). <https://earthdata.nasa.gov/earth-observation-data/near-real-time/download-nrt-data/viirs-nrt#ed-corrected-reflectance>. Accessed 8 Nov 2020
54. Sobrino, J.A., Julien, Y., Soria, G.: Phenology estimation from meteosat second generation data. *IEEE J. Sel. Top. Appl. Earth Obs. Remote Sens.* **6**, 1653–1659 (2013). <https://doi.org/10.1109/JSTARS.2013.2259577>
55. Yan, D., Zhang, X., Yu, Y., Guo, W.: Characterizing land cover impacts on the responses of land surface phenology to the rainy season in the Congo basin. *Remote Sens.* **9** (2017). <https://doi.org/10.3390/rs9050461>
56. Schmid, J.: The SEVIRI instrument (2000)
57. Miura, T., Nagai, S., Takeuchi, M., et al.: Improved Characterisation of vegetation and land surface seasonal dynamics in central Japan with Himawari-8 hypertemporal data. *Sci. Rep.* **9**, 1–12 (2019). <https://doi.org/10.1038/s41598-019-52076-x>
58. Ma, X., Huete, A., Tran, N.N., et al.: Sun-angle effects on remote-sensing phenology observed and modelled using Himawari-8. *Remote Sens.* **12**, (2020). <https://doi.org/10.3390/RS12081339>
59. Yan, D., Zhang, X., Nagai, S., et al.: Evaluating land surface phenology from the advanced Himawari Imager using observations from MODIS and the Phenological Eyes Network. *Int. J. Appl. Earth Obs. Geoinf.* **79**, 71–83 (2019). <https://doi.org/10.1016/j.jag.2019.02.011>
60. eoPortal Directory: Himawari-8 and 9 (2020). <https://directory.eoportal.org/web/eoportal/satellite-missions/h/himawari-8-9>. Accessed 8 Nov 2020
61. Fisher, J.I., Mustard, J.F., Vadeboncoeur, M.A.: Green leaf phenology at Landsat resolution: scaling from the field to the satellite. *Remote Sens. Environ.* **100**, 265–279 (2006). <https://doi.org/10.1016/j.rse.2005.10.022>
62. Melaas, E.K., Friedl, M.A., Zhu, Z.: Detecting interannual variation in deciduous broadleaf forest phenology using Landsat TM/ETM+ data. *Remote Sens. Environ.* **132**, 176–185 (2013). <https://doi.org/10.1016/j.rse.2013.01.011>
63. Liu, J., Heiskanen, J., Aynekulu, E., et al.: Land cover characterization in West Sudanian savannas using seasonal features from annual landsat time series. *Remote Sens.* **8**, 1–18 (2016). <https://doi.org/10.3390/rs8050365>
64. Dethier, B.E., Ashley, M.D., Blair, B., Hopp, R.J.: Phenology satellite experiment. In: Symposium on Significant Results Obtained from the Earth Resources Technology Satellite. Goddard Space Flight Center, New Carrollton, Maryland, pp. 157–165 (1973)
65. eoPortal Directory: Landsat-1 to 8. <https://directory.eoportal.org/web/eoportal/satellite-missions/l/landsat-1-3> (2020). Accessed 8 Nov 2020
66. Solano-Correa, Y.T., Bovolo, F., Bruzzone, L., Fernández-Prieto, D.: Automatic derivation of cropland phenological parameters by adaptive non-parametric regression of Sentinel-2 NDVI time series. *Int. Geosci. Remote Sens. Symp.* 1946–1949 (2018). <https://doi.org/10.1109/IGARSS.2018.8519264>
67. Vrieling, A., Meroni, M., Darvishzadeh, R., et al.: Vegetation phenology from Sentinel-2 and field cameras for a Dutch barrier island. *Remote Sens. Environ.* **215**, 517–529 (2018). <https://doi.org/10.1016/j.rse.2018.03.014>
68. Cai, Z.: Vegetation Observation in the Big Data Era : Sentinel-2 data for mapping the seasonality of land vegetation. Lund University, Faculty of Science (2019)
69. Löw, M., Koukal, T.: Phenology Modelling and Forest Disturbance Mapping with Sentinel-2 time series in Austria (2020)
70. ESA: Sentinel-2 MSI Introduction (2020). <https://sentinel.esa.int/web/sentinel/user-guides/sentinel-2-msi>. Accessed 8 Nov 2020

71. Cheng, Y., Vrieling, A., Fava, F., et al.: Phenology of short vegetation cycles in a Kenyan rangeland from PlanetScope and Sentinel-2. *Remote Sens. Environ.* **248**, 112004 (2020). <https://doi.org/10.1016/j.rse.2020.112004>
72. Myers, E., Kerekes, J., Daughtry, C., Russ, A.: Assessing the impact of satellite revisit rate on estimation of corn phenological transition timing through shape model fitting. *Remote Sens.* **11**, 1–21 (2019). <https://doi.org/10.3390/rs111212558>
73. Sadeh, Y., Zhu, X., Chenu, K., Dunkerley, D.: Sowing date detection at the field scale using CubeSats remote sensing. *Comput. Electron. Agric.* **157**, 568–580 (2019). <https://doi.org/10.1016/j.compag.2019.01.042>
74. Chen, B., Jin, Y., Brown, P.: An enhanced bloom index for quantifying floral phenology using multi-scale remote sensing observations. *ISPRS J. Photogramm. Remote Sens.* **156**, 108–120 (2019). <https://doi.org/10.1016/j.isprsjprs.2019.08.006>
75. Planet: Planet Imagery-Product Specifications. Planet Labs Inc 2018 (2018). <https://www.planet.com/products/planet-imagery/>. Accessed 9 Sept 2020
76. ESA: Planet. eoPortal Dir (2020). <https://directory.eoportal.org/web/eoportal/satellite-missions/p/planet>. Accessed 9 Sept 2020
77. ESA: PlanetScope (2020). <https://earth.esa.int/web/guest/missions/3rd-party-missions/current-missions/planetscope>. Accessed 18 May 2020
78. Gao, F., Anderson, M., Daughtry, C., et al.: A within-season approach for detecting early growth stages in corn and soybean using high temporal and spatial resolution imagery. *Remote Sens. Environ.* **242**, 111752 (2020). <https://doi.org/10.1016/j.rse.2020.111752>
79. Herrmann, I., Bdolach, E., Montekyo, Y., et al.: Assessment of maize yield and phenology by drone-mounted superspectral camera. *Precis. Agric.* **21**, 51–76 (2020). <https://doi.org/10.1007/s11119-019-09659-5>
80. Manivasagam, V.S., Kaplan, G., Rozenstein, O.: Developing transformation functions for VEN μ S and Sentinel-2 surface reflectance over Israel. *Remote Sens.* **11** (2019). <https://doi.org/10.3390/rs11141710>
81. ESA: VEN μ S - Vegetation an Environment monitoring on a New MicroSatellite. *Obs. Earth Environ. Surv. Mission Sensors* (2020). <https://directory.eoportal.org/web/eoportal/satellite-missions/v-w-x-y-z/venus>. Accessed 8 Mar 2020
82. Wulder, M.A., Loveland, T.R., Roy, D.P., et al.: Current status of Landsat program, science, and applications. *Remote Sens. Environ.* **225**, 127–147 (2019). <https://doi.org/10.1016/j.rse.2019.02.015>
83. Storey, J., Roy, D.P., Masek, J., et al.: A note on the temporary misregistration of Landsat-8 Operational Land Imager (OLI) and Sentinel-2 Multi Spectral Instrument (MSI) imagery. *Remote Sens. Environ.* **186**, 121–122 (2016). <https://doi.org/10.1016/j.rse.2016.08.025>
84. Li, J., Roy, D.P.: A global analysis of Sentinel-2a, Sentinel-2b and Landsat-8 data revisit intervals and implications for terrestrial monitoring. *Remote Sens* **9** (2017). <https://doi.org/10.3390/rs9090902>
85. ESA: VEN μ S (Vegetation and Environment monitoring on a New MicroSatellite). eoPortal Dir (2020). <https://directory.eoportal.org/web/eoportal/satellite-missions/v-w-x-y-z/venus>. Accessed 8 Sept 2020
86. Trenkle, T., Driggers, P.: Joint polar satellite system. *Sensors, System Next-Generation Satellite XV* (2019). https://www.jpss.noaa.gov/mission_and_instruments.html. Accessed 18 Sept 2019
87. eoPortal Directory: Satellite Missions Database (2020). <https://eoportal.org/web/eoportal/satellite-missions>. Accessed 3 Dec 2020
88. UrtheCast: UrtheDaily. <https://www.urthecast.com/missions/urthedaily/> (2020). Accessed 9 Sept 2020

89. Fraser, A.D., Massom, R.A., Michael, K.J.: A method for compositing MODIS satellite images to remove cloud cover. *Int. Geosci. Remote Sens. Symp.* **3**, 639–641 (2009). <https://doi.org/10.1109/IGARSS.2009.5417841>
90. Zhu, X., Chen, J., Gao, F., et al.: An enhanced spatial and temporal adaptive reflectance fusion model for complex heterogeneous regions. *Remote Sens. Environ.* **114**, 2610–2623 (2010). <https://doi.org/10.1016/j.rse.2010.05.032>
91. Frantz, D., Stellmes, M., Röder, A., et al.: Improving the spatial resolution of land surface phenology by fusing medium- and coarse-resolution inputs. *IEEE Trans. Geosci. Remote Sens.* **54**, 4153–4164 (2016). <https://doi.org/10.1109/TGRS.2016.2537929>
92. Frantz, D.: FORCE-Landsat + Sentinel-2 analysis ready data and beyond. *Remote Sens.* **11**, 1–21 (2019). <https://doi.org/10.3390/rs11091124>
93. Stellmes, M., Frantz, D., Röder, A., Waske, B.: Multi-annual Phenology Metrics at Landsat Scale in Data-Sparse Areas Fusing annual medium resolution phenology data with ImproPhe. In: 3rd EARSeL SIG LU/LC and NASA LCLUC joint Workshop, Chania (2018)
94. Melaas, E.K., Sulla-Menashe, D., Gray, J.M., et al.: Multisite analysis of land surface phenology in North American temperate and boreal deciduous forests from Landsat. *Remote Sens. Environ.* **186**, 452–464 (2016). <https://doi.org/10.1016/j.rse.2016.09.014>
95. Skakun, S., Roger, J.C., Vermote, E.F., et al.: Automatic sub-pixel co-registration of Landsat-8 Operational Land Imager and Sentinel-2A Multi-Spectral Instrument images using phase correlation and machine learning based mapping. *Int. J. Digit. Earth* **10**, 1253–1269 (2017). <https://doi.org/10.1080/17538947.2017.1304586>
96. Claverie, M., Ju, J., Masek, J.G., et al.: The Harmonized Landsat and Sentinel-2 surface reflectance data set. *Remote Sens. Environ.* **219**, 145–161 (2018). <https://doi.org/10.1016/j.rse.2018.09.002>
97. Claverie, M., Masek, J.G.: Harmonized Landsat-8 Sentinel-2 (HLS) Product User’s Guide (2017)
98. Nijland, W., Bolton, D.K., Coops, N.C., Stenhouse, G.: Imaging phenology; scaling from camera plots to landscapes. *Remote Sens. Environ.* **177**, 13–20 (2016). <https://doi.org/10.1016/j.rse.2016.02.018>
99. Jönsson, P., Cai, Z., Melaas, E., et al.: A method for robust estimation of vegetation seasonality from Landsat and Sentinel-2 time series data. *Remote Sens.* **10**, 1–13 (2018). <https://doi.org/10.3390/rs10040635>
100. Kowalski, K., Senf, C., Hostert, P., Pflugmacher, D.: Characterizing spring phenology of temperate broadleaf forests using Landsat and Sentinel-2 time series. *Int. J. Appl. Earth Obs. Geoinf.* **92**, 1–8 (2020). <https://doi.org/10.1016/j.jag.2020.102172>
101. Li, S., Ganguly, S., Dungan, J.L., et al.: Sentinel-2 MSI radiometric characterization and cross-calibration with Landsat-8 OLI. *Adv. Remote Sens.* **06**, 147–159 (2017). <https://doi.org/10.4236/ars.2017.62011>
102. Chrysafis, I., Mallinis, G., Siachalou, S., Patias, P.: Assessing the relationships between growing stock volume and Sentinel-2 imagery in a mediterranean forest ecosystem. *Remote Sens. Lett.* **8**, 508–517 (2017). <https://doi.org/10.1080/2150704X.2017.1295479>
103. Masek, J., Ju, J., Roger, J., et al.: HLS Operational Land Imager Surface Reflectance and TOA Brightness Daily Global 30 m v2.0. In: NASA EOSDIS L. Process. DAAC (2021). <https://lpdaac.usgs.gov/news/release-of-harmonized-landsat-and-sentinel-2-hls-version-20/>. Accessed 27 Jan 2022
104. Friedl, M., Bolton, D., Moon, M., et al.: MuSLI Multi-Source Land Surface Phenology (MS-LSP) Product User Guide (2020)
105. Eklundh, L., Jin, H., Schubert, P., et al.: An optical sensor network for vegetation phenology monitoring and satellite data calibration. *Sensors* **11**, 7678–7709 (2011). <https://doi.org/10.3390/s110807678>

106. Soto-Berelov, M., Jones, S., Farmer, E., et al.: Chapter 2: Review of validation standards of Earth Observation derived biophysical products. In: *AusCover Good Practice Guidelines: A technical handbook supporting calibration and validation activities of remotely sensed data products*. Pp. 8–30 (2015)
107. Gerstmann, H., Doktor, D., Gläßer, C., Möller, M.: PHASE: a geostatistical model for the Kriging-based spatial prediction of crop phenology using public phenological and climatological observations. *Comput. Electron. Agric.* **127**, 726–738 (2016). <https://doi.org/10.1016/j.compag.2016.07.032>
108. Hess, M., Barralis, G., Bleiholder, H., et al.: Use of the extended BBCH scale - General for the descriptions of the growth stages of mono- and dicotyledonous weed species. *Weed Res.* **37**, 433–441 (1997). <https://doi.org/10.1046/j.1365-3180.1997.d01-70.x>
109. Meier, U.: *Growth stages of mono- and dicotyledonous plants-BBCH Monograph* (2001)
110. Fischer, A.: A simple model for the temporal variations of NDVI at regional scale over agricultural countries. Validation with ground radiometric measurements. *Int. J. Remote Sens.* **15**, 1421–1446 (1994). <https://doi.org/10.1080/01431169408954175>
111. Nasahara, K.N., Nagai, S.: Review: development of an in situ observation network for terrestrial ecological remote sensing: the Phenological Eyes Network (PEN). *Ecol. Res.* **30**, 211–223 (2015). <https://doi.org/10.1007/s11284-014-1239-x>
112. PEN: Phenological Eyes Network (PEN) (2020). <http://www.pheno-eye.org/>. Accessed 11 May 2020
113. Templ, B., Koch, E., Bolmgren, K., et al.: Pan European Phenological database (PEP725): a single point of access for European data. *Int. J. Biometeorol.* **62**, 1109–1113 (2018). <https://doi.org/10.1007/s00484-018-1512-8>
114. PHENOCAM: About the PhenoCam Data (2020). <http://phenocam.us/>. Accessed 12 Nov 2020
115. Zhang, X., Wang, J., Gao, F., et al.: Exploration of scaling effects on coarse resolution land surface phenology. *Remote Sens. Environ.* **190**, 318–330 (2017). <https://doi.org/10.1016/j.rse.2017.01.001>
116. Tang, J., Körner, C., Muraoka, H., et al.: Emerging opportunities and challenges in phenology: a review. *Ecosphere* **7**, 1–17 (2016). <https://doi.org/10.1002/ecs2.1436>
117. Elmendorf, S.C., Jones, K.D., Cook, B.I., et al.: The plant phenology monitoring design for the national ecological observatory network. *Ecosphere* **7**, 1–16 (2016). <https://doi.org/10.1002/ecs2.1303>
118. Tan, B., Gao, F., Tan, B., et al.: An enhanced TIMESAT algorithm for estimating vegetation phenology metrics from MODIS Data. *IEEE J. Sel. Top. Appl. Earth Obs. Remote Sens.* **4**, 361–371 (2011). <https://doi.org/10.1109/JSTARS.2010.2075916>
119. Helman, D., Lensky, I.M., Tessler, N., Osem, Y.: A phenology-based method for monitoring woody and herbaceous vegetation in mediterranean forests from NDVI time series. *Remote Sens.* **7**, 12314–12335 (2015). <https://doi.org/10.3390/rs70912314>
120. Ryu, Y., Lee, G., Jeon, S., et al.: Monitoring multi-layer canopy spring phenology of temperate deciduous and evergreen forests using low-cost spectral sensors. *Remote Sens. Environ.* **149**, 227–238 (2014). <https://doi.org/10.1016/j.rse.2014.04.015>
121. Liang, L., Schwartz, M.D.: Landscape phenology: an integrative approach to seasonal vegetation dynamics. *Landsc. Ecol.* **24**, 465–472 (2009). <https://doi.org/10.1007/s10980-009-9328-x>
122. Bórnez, K., Richardson, A.D., Verger, A., et al.: Evaluation of VEGETATION and PROBA-V phenology using phenocam and eddy covariance data. *Remote Sens.* **12** (2020). <https://doi.org/10.3390/RS12183077>
123. Li, G., Jiang, C., Cheng, T., Bai, J.: Grazing alters the phenology of alpine steppe by changing the surface physical environment on the northeast Qinghai-Tibet Plateau. *China J. Environ. Manage.* **248**, 109257 (2019). <https://doi.org/10.1016/j.jenvman.2019.07.028>

124. Venkatappa, M., Sasaki, N., Shrestha, R.P., et al.: Determination of vegetation thresholds for assessing land use and land use changes in Cambodia using the Google Earth Engine cloud-computing platform. *Remote Sens.* **11**, 1–30 (2019). <https://doi.org/10.3390/rs11131514>
125. Workie, T.G., Debella, H.J.: Climate change and its effects on vegetation phenology across ecoregions of Ethiopia. *Glob. Ecol. Conserv.* **13**, 1–13 (2018). <https://doi.org/10.1016/j.gecco.2017.e00366>
126. Kopp, S., Becker, P., Doshi, A., et al.: Achieving the full vision of earth observation data cubes. *Data* **4** (2019). <https://doi.org/10.3390/data4030094>
127. Li, J., Feng, X., Yin, J., Chen, F.: Change analysis of spring vegetation green-up date in Qinba Mountains under the support of spatiotemporal data cube. *J. Sens.* **2020**, 1–12 (2020). <https://doi.org/10.1155/2020/6413654>
128. Almeida, J., Dos Santos, J.A., Alberton, B., et al.: Applying machine learning based on multiscale classifiers to detect remote phenology patterns in Cerrado savanna trees. *Ecol. Inform.* **23**, 49–61 (2014). <https://doi.org/10.1016/j.ecoinf.2013.06.011>
129. Ryu, D., Kim, T.K., Won, M.S., et al.: Developing a machine learning based automatic plant phenology observation system. In: AGU Fall Meeting Abstracts. AA(Interdisciplinary Program in Agricultural and Forest Meteorology, Seoul National University, Seoul, South Korea), AB(Seoul National University, Seoul, Korea, Republic of (South)), AC(Forest Ecology and Climate Change Division, National Institute of For, pp. B51H-2020 (2018)
130. Czernecki, B., Nowosad, J., Jabłońska, K.: Machine learning modeling of plant phenology based on coupling satellite and gridded meteorological dataset. *Int. J. Biometeorol.* **62**, 1297–1309 (2018). <https://doi.org/10.1007/s00484-018-1534-2>
131. Yuan, H., Wu, C., Lu, L., Wang, X.: A new algorithm predicting the end of growth at five evergreen conifer forests based on nighttime temperature and the enhanced vegetation index. *ISPRS J. Photogramm. Remote Sens.* **144**, 390–399 (2018). <https://doi.org/10.1016/j.isprsjprs.2018.08.013>
132. Yuan, H., Wu, C., Gu, C., Wang, X.: Evidence for satellite observed changes in the relative influence of climate indicators on autumn phenology over the Northern Hemisphere. *Glob. Planet Change* **187**, 103131 (2020). <https://doi.org/10.1016/j.gloplacha.2020.103131>
133. Lu, X., Liu, Z., Zhou, Y., et al.: Comparison of phenology estimated from reflectance-based indices and solar-induced chlorophyll fluorescence (SIF) observations in a temperate forest using GPP-based phenology as the standard. *Remote Sens.* **10** (2018). <https://doi.org/10.3390/rs10060932>
134. Wang, X., Dannenberg, M.P., Yan, D., et al.: Globally consistent patterns of asynchrony in vegetation phenology derived from optical, microwave, and fluorescence satellite data. *J. Geophys. Res. Biogeosciences* **125**, 1–15 (2020). <https://doi.org/10.1029/2020JG005732>
135. Eklundh, L.: Welcome to the TIMESAT pages! TIMESAT (2017). <http://www.nateko.lu.se/TIMESAT/timesat.asp>. Accessed 25 Sep 2019
136. Rodrigues, A., Marcal, A.R.S., Cunha, M.: Monitoring vegetation dynamics inferred by satellite data using the PhenoSat tool. *IEEE Trans. Geosci. Remote Sens.* **51**, 2096–2104 (2013). <https://doi.org/10.1109/TGRS.2012.2223475>
137. Marcal, A.R.S., Cunha, M.: PhenoSat (2020). <https://www.fc.up.pt/PhenoSat/software.html>. Accessed 3 Mar 2020
138. Verbesselt, J., Hyndman, R., Newnham, G., Culvenor, D.: Detecting trend and seasonal changes in satellite image time series. *Remote Sens. Environ.* **114**, 106–115 (2010). <https://doi.org/10.1016/j.rse.2009.08.014>
139. Masters, P., Gehrt, J., Keast, R., et al.: Statistical Analysis of Grassland Trends and Phenology using Satellite Time Series Imagery of the Flint Hills Ecoregion. Manhattan (2016)

140. Hutchinson, J.M.S., Jacquin, A., Hutchinson, S.L., Verbesselt, J.: Monitoring vegetation change and dynamics on U.S. army training lands using satellite image time series analysis. *J. Environ. Manage.* **150**, 355–366 (2015). <https://doi.org/10.1016/j.jenvman.2014.08.002>
141. Rembold, F., Tote, C., Eerens, H., et al.: SPIRITS. Addis Ababa, Ethiopia (2013)
142. Rembold, F., Meroni, M., Urbano, F., et al.: Remote sensing time series analysis for crop monitoring with the SPIRITS software: new functionalities and use examples. *Front. Environ. Sci.* **3**, 1–11 (2015). <https://doi.org/10.3389/fenvs.2015.00046>
143. Eerens, H., Haesen, D., Rembold, F., et al.: Image time series processing for agriculture monitoring. *Environ. Model Softw.* **53**, 154–162 (2014). <https://doi.org/10.1016/j.envsoft.2013.10.021>
144. Eerens, H., Dominique, H.: Software for the Processing and Interpretation of Remotely sensed Image Time Series USER'S MANUAL Version : 1.1.1 (2013)
145. Bornez, K., Verger, A., Filella, I., Penuelas, J.: Land surface phenology from Copernicus Global Land time series. In: 2017 9th International Workshop on the Analysis of Multitemporal Remote Sensing Images, MultiTemp 2017, vol. 1, pp. 17–20 (2017). <https://doi.org/10.1109/Multi-Temp.2017.8035262>
146. Forkel, M., Carvalhais, N., Verbesselt, J., et al.: Trend change detection in NDVI time series: effects of inter-annual variability and methodology. *Remote Sens.* **5**, 2113–2144 (2013). <https://doi.org/10.3390/rs5052113>
147. Forkel, M., Migliavacca, M., Thonicke, K., et al.: Codominant water control on global interannual variability and trends in land surface phenology and greenness. *Glob. Change Biol.* **21**, 3414–3435 (2015). <https://doi.org/10.1111/gcb.12950>
148. Forkel, M., Wutzler, T.: Greebrown - land surface phenology and trend analysis. A package for the R software. Version 2.2 (2015). <http://greenbrown.r-forge.r-project.org/>
149. Lange, M., Doktor, D.: Package 'phenex' (2017)
150. Nativi, S., Mazzetti, P., Santoro, M.: Deliverable No : D10.1 Design of the ECOPOTENTIAL Virtual Laboratory, Version V1.0 (Final Draft) (2016)
151. Guigoz, Y.: Estimation of phenology metrics (PhenologyMetrics) - ECOPotential Virtual Laboratory - ESSI Lab Documentation (2017). <https://confluence.geodab.eu/pages/viewpage.action?pageId=2458817>. Accessed 25 Sept 2019
152. Gray, J., Sulla-Menasche, D., Friedl, M.: Lp Daac - Mcd12Q2 (2019). <https://lpdaac.usgs.gov/products/mcd12q2v006/>. Accessed 26 Sept 2019
153. USGS: VIPPHEN_NDVI v004 (2019). https://lpdaac.usgs.gov/products/vipphen_ndvi_v004/. Accessed 7 Jan 2020
154. Bolton, D., Gray, J.M., Melaas, E.K., et al.: Continental-scale land surface phenology from harmonized Landsat 8 and Sentinel-2 imagery. *Remote Sens. Environ.* **240**, 1–16 (2020). <https://doi.org/10.1016/j.rse.2020.111685>